

# Out-of-Plane Behavior of Brick Masonry Walls Strengthened with Fiber Composites

Juan I. Velazquez-Dimas, Mohammad R. Ehsani, and Hamid Saadatmanesh

*The vulnerability of unreinforced masonry buildings (URM) to moderate ground motions is a fact recognized by the earthquake engineering community. In this paper, an innovative retrofitting system for URM buildings using glass fiber reinforced polymer (GFRP) strips is investigated. The experimental results for four retrofitted URM walls subjected to cyclic out-of-plane loading are presented herein. The first three specimens were constructed in single wythe, and the fourth one in double wythe. The height-thickness ratio for all specimens was 28. Depending on the reinforcement ratio, single wythe walls failed in tension, excessive delamination, or a combination of both. Failure modes in the double wythe wall were peeling off of composite strips and splitting of the wythes. From experimental results, it was found that walls were capable of supporting pressures of up to 25 times their weight and deflect up to 1/20 times the wall height. Strength and deformation capacity of the walls were significantly improved by the investigated retrofitting technique.*

**Keywords:** flexural strength; masonry; prestressing steel; reinforced concrete; stiffness

## INTRODUCTION

Unreinforced masonry buildings (URM) constitute a large portion of the world's building inventory. The vulnerability of these structures to moderate seismic forces is a fact recognized by earthquake engineers. Forming part of this stock are the most appreciated historical monuments, which need to be preserved. As an example, more than 20,000 URM buildings exist in California alone. Most of these were constructed considering little, if any, seismic design criteria (Laurence 1984; Reinhorn et al. 1985; Abrams 1988; Bruneau 1994a; Sucouglu et al. 1996). Old masonry buildings are primarily composed of load-bearing walls constructed with solid or hollow clay brick. Masonry walls are commonly attached to either flexible (wood) or rigid (concrete) diaphragms. In the event of an earthquake, these structural elements transfer the seismic forces to the foundation. Due to a weak anchoring system or lack of reinforcement, load-bearing walls may tear from the building or collapse under in-plane or out-of-plane forces.

In recent earthquakes, some URM buildings that were retrofitted earlier performed well. Some others that were strengthened (more than 450) with current design procedures, however, were damaged during the Northridge earthquake (Kehoe 1996). These figures suggest that actual masonry behavior is not properly considered in the retrofitting schemes. In addition, the seismic demand for out-of-plane loads in the UBC code has increased by as much as 50% during the last 20 yr (Bhende et al. 1994; Wong 1994). Therefore, there is a need for better understanding of brickwork behavior under reversed loads, and the development of new and more efficient strengthening techniques.

The objective of this study is to investigate the flexural behavior of slender URM walls retrofitted with vertical glass fabric composite strips and subjected to cyclic out-of-plane loading. The influence of the number of wythes on the behavior of the walls is also investigated. This study is part of a larger investigation that was presented in two other publica-

tions (Ehsani et al. 1999; Velazquez-Dimas and Ehsani 2000).

## PERFORMANCE OF URM WALLS

As mentioned previously, masonry walls may fail under in-plane or out-of-plane forces. Significant research has been published for in-plane behavior of URM masonry walls (Sucouglu et al. 1991; Mengy et al. 1989; Abrams 1986). There are not enough data, however, for URM walls under out-of-plane loading (Hendry 1973; Essaway 1986; Dawe et al. 1989; Drysdale et al. 1994). The more significant retrofitting techniques reported to enhance flexural capacity of masonry walls are: shotcreting reinforced with steel mesh; bonding steel plates; prestressing; center core technique; and bonding composite fabrics or plates. In the following paragraphs, some of the most important studies on flexural behavior of slender URM walls retrofitted with different surface treatment techniques are discussed. Additional details for other types of retrofitting procedures can be found elsewhere (Velazquez-Dimas 1998).

Bhende and Ovidia (1994) tested eight walls, each 203 mm (8 in.) thick, 1200 mm (48 in.) wide, and 2600 mm (104 in.) high. The specimens were retrofitted by attaching a 16 x 150 mm (0.675 x 6.0 in.) steel plate to each face of the walls using four through-bolts at the top and bottom of the wall. The specimens were subjected to static out-of-plane loading. From experimental results, they found that the out-of-plane capacity of the walls was increased by a factor of 10. They suggested, however, that further studies are needed to investigate the effect of the drilled holes on the in-plane capacity of the wall.

Dawe and Aridru (1993) demonstrated that cracking capacity, ultimate strength, and ductility of plane masonry walls can be enhanced with prestressing bars. They tested two series of five full-scale specimens, each 1200 mm wide, 3000 mm high, and 140 and 190 mm thick. The specimens were subjected to monotonic out-of-plane loading applied with an air-bag system. Experimental results showed a significant increase in the wall stiffness of prestressed walls compared with traditionally reinforced masonry. An equation to estimate the flexure capacity of the prestressed walls was also presented.

Prawel and Reinhorn (1985) proved that a thin bonded coat of reinforced cement to one or both sides of a masonry panel could substantially improve the in-plane and out-of-plane strength and ductility. They showed that for in-plane loading of URM panels, the strength, ductility, and stiffness of the retrofitted specimens were almost twice of the bare specimens. A number of other studies have also been carried out on masonry buildings (Clough et al. 1990; Sveinsson et al. 1988; ABK 1981).

The application of fiber composites in the repair and rehabilitation of structures has become popular (Saadatmanesh

*ACI Structural Journal*, V. 97, No. 3, May-June 2000.

MS No. 99-036 received March 9, 1999, and reviewed under Institute publication policies. Copyright © 2000, American Concrete Institute. All rights reserved, including the making of copies unless permission is obtained from the copyright proprietors. Pertinent discussion will be published in the March-April 2001 *ACI Structural Journal* if received by November 1, 2000.

**Juan I. Velazquez-Dimas** is a Professor of Civil Engineering at Universidad Autonoma de Sinaloa, Culiacan, Mexico. He received his PhD from the University of Arizona in 1998. His research interests include the use of composite materials in the rehabilitation of infrastructure.

**Mohammad R. Ehsani, FACI**, is Professor of Civil Engineering and Engineering Mechanics at the University of Arizona. His research interests include repair and rehabilitation of the infrastructure with fiber composites, and nondestructive evaluation of structures.

ACI member **Hamid Saadatmanesh** is a professor of civil engineering at the University of Arizona, Tucson. His research interests include the application of advanced fiber composites for repair and rehabilitation of structures. He is the past secretary and current member of ACI Committee 440, Fiber Reinforced Polymer Reinforcement.

and Ehsani 1996 and 1998). In recent years, many researchers have used composite materials in the form of fabrics or composite plates to retrofit URM walls against in-plane and out-of-plane loads (Laursen et al. 1995; Schwegler and Kelterborn 1996; Ehsani and Saadatmanesh 1994, 1996, and 1997; Reinhorn and Madan 1995). Velazquez-Dimas et al. (1998) reported that strength and deformation capacity of URM walls retrofitted with glass fabric composite strips can be substantially enhanced. Deflections up to 4% of the wall span can be reached. The ultimate pressure supported by the tested walls can be up to 31 times the weight of the wall.

## EXPERIMENTAL PROGRAM

### Description and construction of specimens

Four half-scale slender masonry walls were constructed by an experienced mason using solid clay bricks. The brick units were cut from pavement solid clay bricks supplied by a local manufacturer. The half-scale units had dimensions of 49 x 38 x 102 mm (1.92 x 1.5 x 4 in.). The units were bonded with a low-strength capacity Type N mortar. All specimens had the same height-thickness ratio of 28. Three of the tested walls were constructed in single wythe. The fourth wall was constructed in double wythe, with a header course placed every six courses. This frequency of header course has been used in a large number of older URM buildings. Bricks were bonded in running bond pattern with a mortar joint of a 1/4 in. thickness to match the reduced-scale brick dimensions. To scale the sand for this mortar thickness, the following percentage passing were used for the various sieve sizes: No. 18: 95%, No. 30: 67%, No. 50: 24%, No. 100: 6%, No. 140: 3%, and No. 200: 2%. The main geometric features of the constructed walls are illustrated in Table 1.

The advantages of using scaled masonry specimens have been outlined by many researchers (Abboud et al. 1990; Sinha et al. 1970). Other researchers have also successfully studied scaled masonry structures (Hendry 1973; Abrams 1988; Abrams et al. 1996).

The first course of bricks for the four walls was laid in a machined steel channel that formed part of the support during the test. As can be observed in Fig. 1, all walls were simply supported at the top and bottom, and the other two sides remained free. With these boundary conditions, it was intended to simulate the portion of the masonry walls found in low-rise buildings free of corner and wall-to-wall joint interference.

Each wall was designated with a letter followed by one or two numbers. The letter S refers to single wythe, and the letter D to

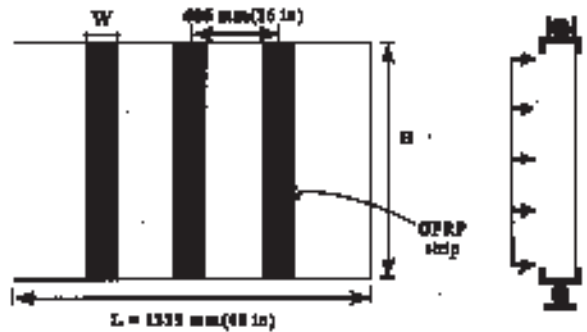


Fig. 1 Overall view of the test specimen.

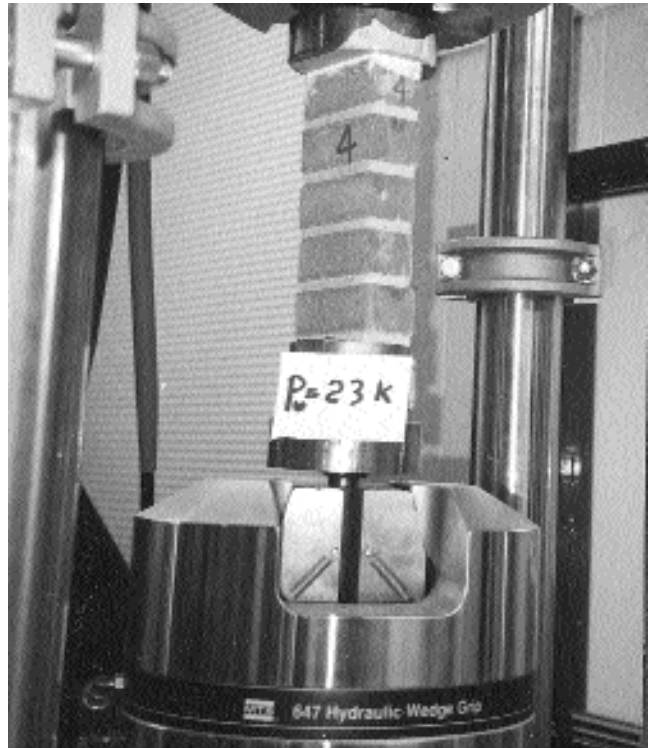


Fig. 2 Test of brick prisms for determination of compression capacity of brickwork.



(a)



(b)

Fig. 3 Steps in retrofit procedure: (a) spreading the epoxy over the fabric; (b) bonding the fabric to the wall.

Table 1—Overall wall parameters

Specimen Designation	Length mm (in.)	Height mm (in.)	h/t	%ρ <sub>s</sub>		Fabric Width (W) mm (in.)		w/t	
				South face	North face	South face	North face	South face	North face
S100/100	1220 (48)	1420 (56)	28	100	100	135 (5.3)	135 (5.3)	2.76	2.76
S300/300	1220 (48)	1420 (56)	28	300	300	406 (16)	406 (16)	8.3	8.3
S50/200	1220 (48)	1420 (56)	28	50	200	67 (2.65)	270 (10.6)	1.4	5.5
D100	1220 (48)	2740 (108)	28	0	100	0	280 (11)	—	2.75

W = fabric width; h = height; and t = thickness; S = single wythe; D = double wythe; and ρ<sub>s</sub> = reinforcement ratio

Table 2—Material properties

Component	Measured property	Measured values For single wythe walls	Measured values For double wythe wall
Brickwork	Density kN/m <sup>3</sup> (lb/ft <sup>3</sup> )	18.7 (120)	18.7 (120)
Brick units	Compression capacity MPa (ksi)	45 (5.1)	45 (5.1)
	Initial rate of absorption gm/min	7.9	7.9
Mortar	Compression capacity kPa (psi)	5190 (754)*	5826 (845)*
		7200 (1044)**	
Brick prisms	Compression capacity MPa (ksi)	20 (2.9)*	26 (3.767)*
		26.7 (3.87)**	
Brick beams	Modulus of rupture kPa (psi)	1482 (215)*	1124 (163)*
		1613 (234)**	

\*Determined at 28 days

\*\*Determined at testing time.

double wythe. The designation for S series specimens is followed by two numbers that refer to the percentage of the composite reinforcement on the south and the north faces of the wall with respect to the balanced condition used, respectively. A number indicating the reinforcement ratio for the north face follows the letter D. The four walls were strengthened with strips of a fabric constructed with E-glass, in which the glass fibers were aligned vertically (i.e., along the height of the wall). The fabric was bonded to the wall surface with a two-component epoxy resin. The balanced condition is

assumed to occur when the compressive failure of the masonry is reached at the same time that the composite fails in tension.

### Material properties

All material properties were determined according to the appropriate ASTM standard. The compression capacity, initial rate of absorption (IRA), and the density were determined for brick units. From test results, it was found that brick units needed to be wet to improve the bond between the mortar and

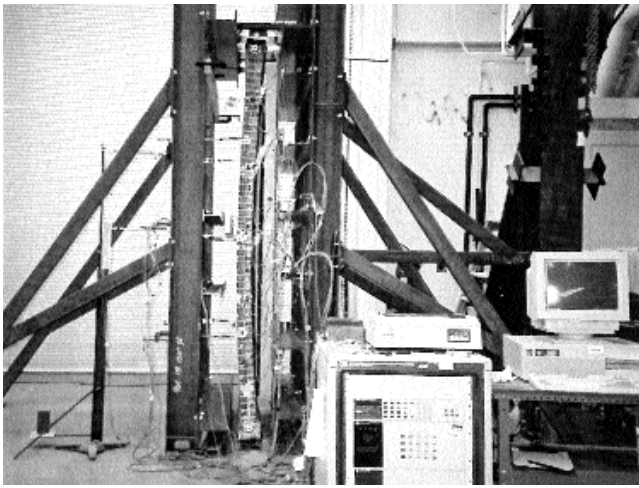


Fig. 4 Test setup.

the bricks. From prisms constructed with five bricks, the compressive capacity of the brick-mortar assemblage was determined. Figure 2 shows a typical test specimen. The modulus of rupture for brickwork was also determined from brick beams constructed with 10 bricks. The last properties were determined at 28 days and at testing time, as shown in Table 2. The density for brick-mortar assemblages was determined from coupons for modulus of rupture. From mortar cubes of 50 x 50 x 50 mm (2 x 2 x 2 in.), the mortar compression capacity was also obtained at 28 days and at testing time for all specimens. A sieve analysis was carried out for the sand used in the mortar. Using sand from river passing mesh No. 8, a 1/4 in. mortar bed joint was used to match the half-scale bricks used in this investigation. A unidirectional glass fabric weighing 18 oz per yd<sup>2</sup> was used for retrofitting all the walls. The tensile strength of the composite fabric was obtained according to ASTM D-3039 to be 369 N/mm (2106 lb/in.) width based on the average of six coupons.

### Retrofitting procedure

The single wythe specimens were retrofitted with three vertical strips of glass fabric bonded on the north and the south wall faces. The double wythe wall was strengthened on the north face only. The composite strips were bonded with an epoxy resin using the wet layup procedure. A more detailed description of the steps involved in retrofitting a wall with fiber composites is given elsewhere (Ehsani and Saadatmanesh 1996). It is noted that, similar to many other construction practices, this technique has been patented (Lester 1998; Ehsani and Saadatmanesh 1997). The wall was first cleaned with a steel brush, then dust and any loose particles were removed with high air pressure. A thin layer of primer was coated to the wall surface where the composite strips were to be attached (for all walls except for Wall S100/100). Next, the composite strips were cut to size and laid on a plastic sheet and the mixed epoxy was poured on the fabric and spread over the whole fabric, ensuring that the fabric was saturated with the epoxy. The saturated composite strips were bonded to the wall face by hand pressure and pressed with a roller (Fig. 3). Finally, the exterior surface of the fabric was coated with a small layer of epoxy for protection and instrumentation purposes. The four walls were retrofitted following the same procedure. As depicted in Fig. 1, the center-to-center space between the vertical strips was kept constant at 406 mm (16 in.) for all walls. The fabric width varied for different reinforcement ratios. The values are shown in Table 1.

There are a number of reported field applications where fiber composites have been used to strengthen buildings and

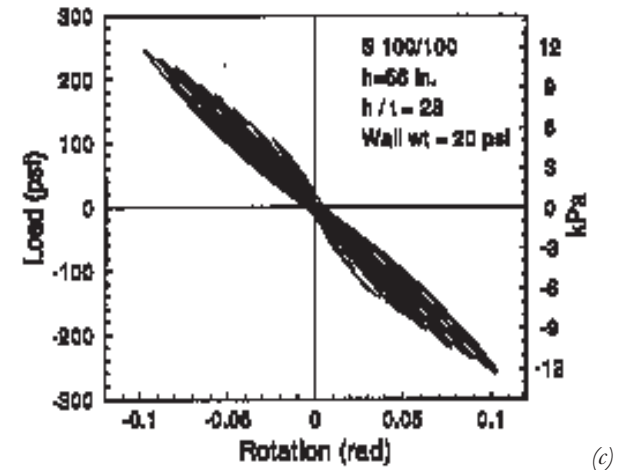
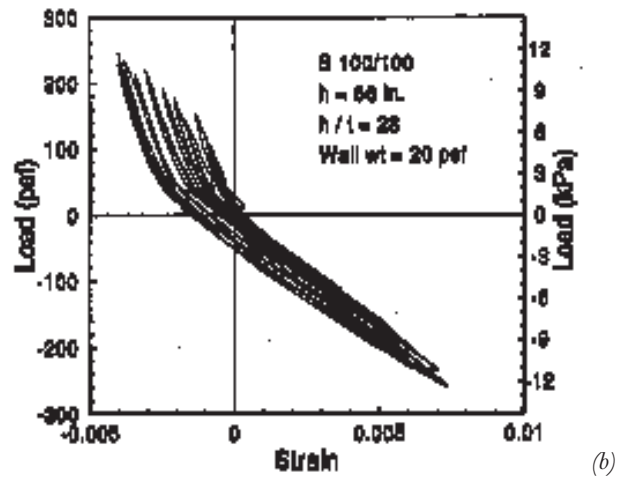
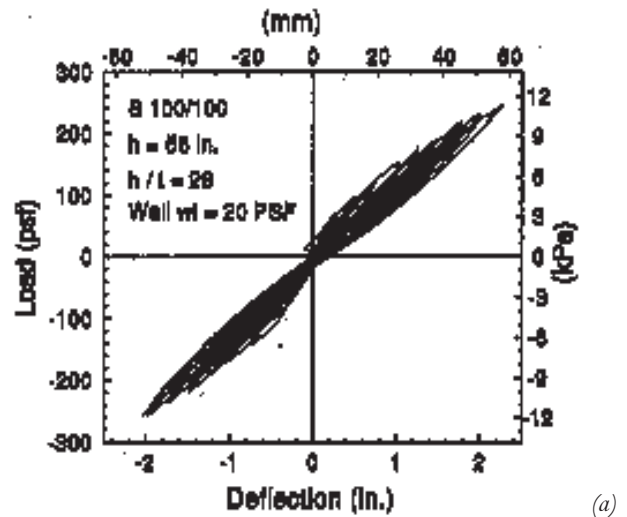


Fig. 5 Typical measurements for Specimen S 100/100: (a) load versus deflection at mid-height; (b) load vs. the longitudinal strain in the composite strip; and (c) load versus rotation at the top support.

bridges (Saadatmanesh and Ehsani 1996 and 1998). In many cases, these structures have been in service for several years with no apparent sign of damage or deterioration to the composite. The durability of composites in other industries, such as boat building and aerospace, is well documented. Clearly, as the collective experience of the construction industry with the performance of these materials increases over the coming years, advances will be made towards the elimination of any shortcomings that these systems may have.

Table 3—Summary of the observed behavior of the tested walls

Table 3. Summary of the observed behavior of the tested walls

DESIGNATION		S100/100		S300/300		S50/200		D100
Face		S	N	S	N	S	N	N
Reinforcement ratio (%)		100	100	300	300	50	200	100
First major crack	Cycle	9	8	7	7	6	6	7
	Pressure, kPa (psf)	4.62 (97)	4.62 (97)	10.34 (216)	13.1 (274)	2.81 (59)	8.7 (187)	4.6 (97)
	Deflection mm (in.)	12.3 (0.5)	12.5 (0.5)	12.3 (0.5)	14 (0.56)	10 (0.4)	14 (0.56)	15 (0.59)
	Location	Above and below middle brick course	Above and below middle brick course	Below middle brick course	At mid-height on west edge	Above middle brick course	Two courses above middle brick course	At mid-height and below up to 5 courses
First delamination	Cycle	13	14	11	11	9	13	9
	Pressure kPa (psf)	6.9 (144)	7.6 (158)	17 (360)	18.34 (383)	3.75 (78)	13.3 (274)	5.3 (112)
	Deflection mm (in.)	25 (1.0)	25 (1.0)	25 (1.0)	25 (1.0)	21 (0.86)	33 (1.3)	20 (0.79)
	Location	Central strip above mid-height	Central strip above mid-height	At center around an air bubble	At center around an air bubble	West and east strips above	West and east strips at mid-height	Central and west strips at center and 18" above
Maximum strain (%)	Comp. †	0.4	0.4	0.19	0.3	0.3	0.2	0.12
	Tension	0.9	1.0	0.4	0.5	1.3	1.1	0.8
	Strip	West and east at center	Central at mid-height	At center at middle brick course	At center at middle brick course	West at center	Central and west at center	East at 18" below middle brick course
Maximum rotation (°)	Top	6	6	3.4	3.4	3.7	7.4	4.6
Mode of Failure	Cycle	23	23	13	12	25	27	24
	Pressure kPa (psf)	11.7 (243)	11.71 (243)	22.75 (473)	16.7 (350)	6.2 (130)	20.7 (432)	9.8 (205)
	Deflection mm (in.)	56 (2.3)	58 (2.3)	33 (1.3)	25 (1.0)	47 (1.84)	70 (2.75)	76 (3.0)
	Type	FD	T, FD	SHEAR	No Failure	T, PD	C, FD	FD
	Location	All strips 70% delam. Areas	All strips ‡	At bottom brick course	No	West strip 90% delam.	All strips †	All strips †
Span drift $\delta_{max}/h$ (%)		4.0	4.0	2.3	2.0	3.4	5.0	2.77
$P_{max}/Wt$		13	13	24	17.5	7	23	5

NOTES: D = Delamination, T = Tension, C = Compression, Wt = Weight of the wall/ft<sup>2</sup>

FD and PD = Full and Partial Delamination

† Compression strains were measured on the composite fabric.

‡ Central and west strips on top half and the east strip at midheight.

†† Central and east strips from top support to midway of the bottom half part and the west strip from top midway to the bottom support. All strips delaminated almost 70%. A compression failure was also observed on the south face.

††† All strips delaminated almost 80%. Symmetrical delaminated patterns were observed for the three strips.

### Testing frame

The four walls were tested in a steel reaction frame. The specimens were simply supported along the top and the bottom edges, and the two vertical sides were free. With these boundary conditions, it was intended to reproduce a portion of the wall free of corner and joint interference. A roller condition was provided at the top, i.e., vertical displacements and rotations were allowed. The specimens were subjected to cyclic out-of-plane loading. The lateral pressure was applied through an airbag system that was moved from one face of the wall to the other; more details about the test setup are presented elsewhere (Velazquez-Dimas 1998). The load was applied to the walls in two stages: a load-controlled stage, which consisted of two pairs of cycles to observe the uncracked behavior; and a displacement-controlled stage,

where the maximum displacement in each pair of cycles remained constant. The stiffness degradation was monitored using two loading cycles for the same displacement level. This procedure was continued until the failure of the wall was reached. To exclude the beneficial effect of overburden pressure, no axial load was applied to the specimens. An overall view of the testing frame showing the double wythe wall is given in Fig. 4. The maximum deflection at midheight of the west edge and the applied pressures were monitored in real time by two voltmeters, and the corresponding load versus deflection curves were plotted on the monitor of the data acquisition system.

### Instrumentation

The specimens were instrumented with several devices. Ten strain gages were bonded to the north and the south faces

of the single wythe walls to measure longitudinal and transverse strains. The double wythe wall was instrumented differently since it was retrofitted on one face only. Thus, 17 strain gages were bonded to the composite strips and three strain gages were bonded at midheight on the south face of the wall to measure compressive strains on the brick surface. Five clinometers were attached to the east and the west sides of the four walls to measure rotations. In addition, seven points were instrumented on all specimens with linear variable displacement transducers (LVDTs) to measure out-of-plane deflections of the wall surface. The applied pressure to the wall surface was measured with an electronic pressure sensor capable of reading pressure increments of 345 Pa (0.05 psi). The information read by each device was recorded using a computer-controlled data acquisition system. Finally, vertical gypsum strips were built around the midheight portion of the specimens on the south and the north wall faces for detection of bed joint cracks.

## EXPERIMENTAL RESULTS

A summary of the observed behavior of the tested walls is presented in Table 3. In this part, a detailed description of the behavior of Specimen S100/100 is given. This is followed by a general discussion of the other walls. More detailed information about the behavior of the tested walls can be found in Velazquez-Dimas (1998).

### Wall S100/100

This wall was symmetrically strengthened with three vertical composite strips, each 135 mm (5.3 in.) wide. This reinforcement ratio was equivalent to balanced condition, i.e., a tensile failure in composite strips would occur at the same time that the masonry failed in compression. These calculations were made assuming linear strain variation along the depth of the wall and using mechanical properties obtained from compressive tests of the masonry prisms and tensile coupon tests of the composite material. Additional description of these calculations and the predicted behavior of the specimens is presented elsewhere (Velazquez-Dimas and Ehsani 2000). No primer was used in this wall to improve interface behavior of the composite strips. The wall was subjected to 23 cycles of loading. For the first 20 cycles, cracking and delamination patterns were fairly symmetrical on both faces. The observed behavior of this wall is explained as follows.

The first major visible crack along a bed joint was detected on the north face during the eighth cycle at an applied pressure of 4.62 kPa (96.5 psf), and at a deflection of 12.5 mm (0.5 in.). These cracks were marked at midheight immediately above and below the middle mortar joint. Upon reversal of loading, the same type of crack was observed on the south face of the wall at similar load and displacement levels. Significant stiffness degradation was observed after the major crack. The enlarged hysteretic loop areas following a displacement of 12.5 mm in Fig. 5(a) is attributed to this. Full longitudinal bed joint cracks formed above and below the middle brick course more or less in a uniform pattern. As pressures reached higher levels, mortar joint cracks grew up in number, as well as in size, toward the top and the bottom supports.

Delamination is another factor that produces loss of stiffness. The first delaminated areas were observed on the north face during the fourteenth cycle at an applied pressure of 7.6 kPa (158 psf), and a deflection of 25 mm (1.0 in.). These delaminated areas were marked on the central composite strip above the middle brick course. Delaminated areas are often accompanied by sounds of the epoxy breaking away from the brick surface, and result in enlarged hysteretic loops. Similar behavior was observed for the south face as shown in Table 1, where close correlation is shown for both faces. In Fig. 5(a),

the first significant stiffness degradation seemed to be more influenced by the formation of large cracks along bed joints rather than the formation of the first delaminated areas. After these two major damages occurred, the additional cycles of loading resulted in further delamination of the fabric strips.

As mentioned previously, fairly symmetrical behavior was observed for both wall faces. This was also observed for longitudinal strains. Longitudinal tensile strains as much as 1% were measured in the composite strips at midheight on both wall faces. From tensile coupon tests according to ASTM D-3039, composite strips should reach a minimum longitudinal strain of 1.5% prior to failure. Although a tensile failure occurred on the north composite strips, an ultimate strain of 1.5% could not be reached. This is attributed to the fact that composite strips are subjected to a complex combination of loads including longitudinal, transverse, and shear. Figure 5(b) shows a load-versus-longitudinal tensile strain curve for a strain gage bonded on the north central composite strip at midheight. A maximum longitudinal compressive strain of 0.4% was also measured on the composite strip for the south and the north faces. In addition, transverse strains were measured at midheight on the three composite strips. From the collected data, it was found that transverse strains as much as 500 microstrain were measured, indicating that transverse stresses on composite strips were very small; however, such strains could contribute to the delamination of the composite fabric.

Rotations on the west and the east wall edges of the wall were also measured. From the recorded data, this wall rotated at the top and the bottom supports up to 6 degrees. This gave an indication of how the composite strips can transform a brittle wall into a flexible one. In Fig. 5(c), a typical load-versus-rotation curve is depicted for a clinometer attached to the top west corner. This curve also confirms the symmetry that was mentioned previously. In addition, measured rotations at midheight were almost zero, indicating that the pressure applied by the airbag system was symmetrical.

Tensile failure occurred on all three north composite strips. Prior to the fracture of the north strips, cracking sounds indicated the imminent failure. While the central and the west strips failed above the middle brick course, the east strip broke at midheight. Although the balanced reinforcement ratio suggests simultaneous tension and compression failure of the wall, no compression failure of the brick was observed. This may be attributed to the uneven wall surface that would create local stress concentration points at the edges of each brick. Due to the failure on the north face, the composite strips of the south face did not fail. A vertical crack passing through the brick was detected underneath the central strip at failure. This indicated that the flexural capacity of the brickwork perpendicular to the bed joint was reached. Therefore, a minimum amount of horizontal reinforcement needs to be provided to avoid such failure.

In summary, the behavior of the wall was characterized by excessive cracking along the mortar joints all over the north and the south wall surfaces. The crack patterns on both faces seemed more or less uniformly distributed. Extensive delamination also took place on the composite strips on both faces. By the conclusion of the test, delaminated areas covered approximately 75% of the entire area of the strips. Delaminated patterns, however, were nonsymmetrical for the two faces. On the north face where tensile failure occurred, the east strip delaminated fairly symmetrically above and below the middle brick course. The central and west strips, however, delaminated from the bottom, midway to the top support. The wall was subjected to 23 cycles of loading, supported a maximum lateral pressure of 11.7 kPa (249 psf), and deflected 58 mm (2.3 in.). The failure load was equivalent to

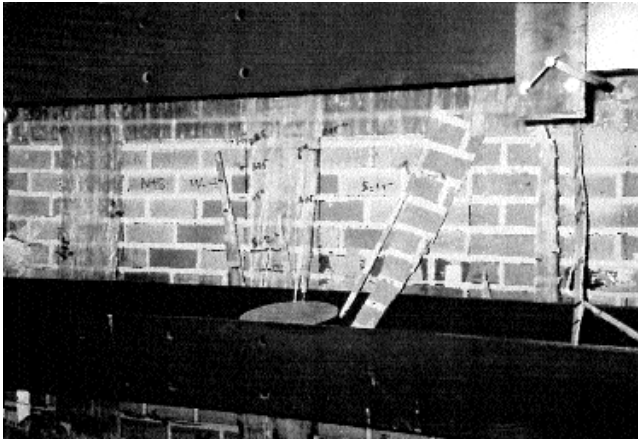


Fig. 6 Failure of the composite strips on the north face of Specimen S100/100.

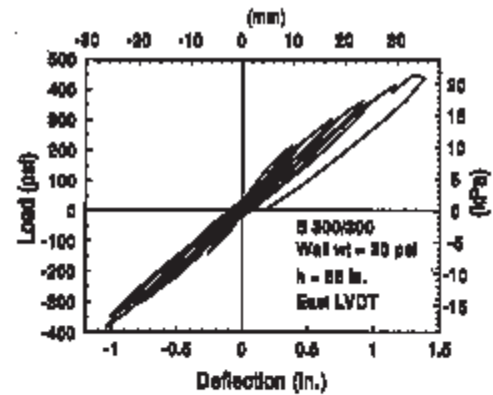
nearly 13 times the weight of the wall, and the maximum deflection was almost 4% of the span. Figure 6 shows the failed north composite strips.

### Wall S300/300

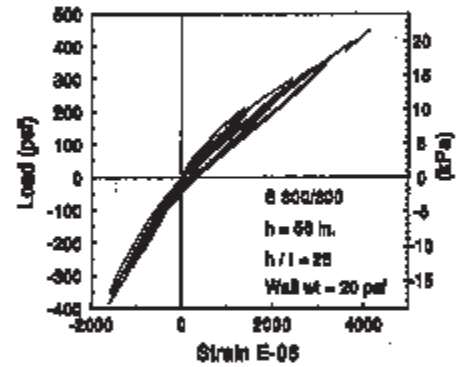
Based on the observed results of the previous wall, it was decided to test the next wall with a higher reinforcement ratio. The wall surfaces on both faces were fully covered with the same fabric, i.e., an 18 oz per  $\text{yd}^2$  unidirectional glass fabric. This resulted in a reinforcement ratio equivalent to three times the balanced condition. As expected, very stiff behavior was observed for this wall. Almost linear elastic behavior was observed because of the high reinforcement ratio used. This behavior can be seen in Fig. 7, where typical curves for deflection, strain, and rotations are depicted. Little damage was observed for this wall. The few delaminated areas that were marked on either faces of the wall were initiated by the presence of air bubbles that were introduced by entrapped air during the bonding of the fabric. The measured compressive strains in the composite fabric were very close to the calculated values for the brick; this indicates that good interface bond existed between the two materials. Very small bed-joint cracks also developed. Since the fabric covered the entire wall surface, it was very difficult to detect bed-joint cracks. These were marked only at the vertical edges. Initial cracks were detected on vertical strips of gypsum that were bonded to the fabric surfaces on both faces. Because the wall suffered little damage, very narrow hysteric loops were observed, and hence, little energy was dissipated.

The failure occurred during the thirteenth cycle while pushing from the north face at an applied pressure of 22.8 kPa (475 psf). This was characterized by formation of a fully longitudinal crack through the bottom brick course, indicating shear failure of the brick. In fact, as expected, due to the high reinforcement ratio, no tension failure of the composite strips or compression failure of the bricks occurred. This is evident by the maximum tensile strain in the composite reaching 0.4%. Since the applied shear stresses at the supports were approximately 344 kPa (50 psi), the shear capacity of the brickwork was exceeded according to the UBC and the ACI/ASCE/TMS specifications. Figure 8 shows the failure of the wall.

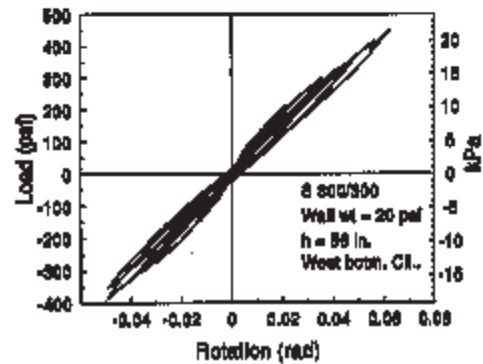
In summary, the wall supported lateral pressures equivalent to almost 24 times its own weight. The maximum measured deflection was equivalent to 1/50 times the wall span. According to the latest masonry specifications, this deflection



(a)



(b)



(c)

Fig. 7 Typical measurements for Specimen S300/300: (a) load versus deflection at midheight; (b) load versus the longitudinal strain in the composite strip; and (c) load versus rotation at the bottom support.

was almost 13 times the allowable value if the wall was unreinforced.

### Wall S50/200

To get as much information as possible about the behavior of this type of masonry walls and based on results from the previous two symmetrical specimens, it was decided to retrofit this wall in a nonsymmetrical way. Thus, reinforcement ratios of 1/2 and two times the balanced condition were used on the south and the north wall faces, respectively. As a result, the three wall specimens would provide information on the behavior of systems retrofitted with four different reinforcement ratios.

Excessive bed-joint cracking and delamination of the composite strips characterized the observed behavior on both wall faces. Bed-joint cracks spread to almost 90% of the wall surface. Cracks went through almost 80% of the wall thickness.

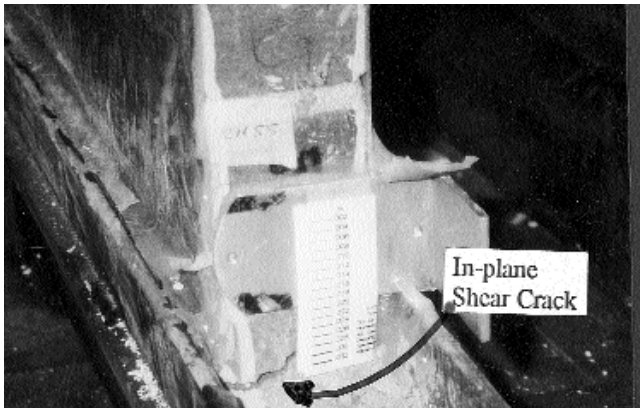


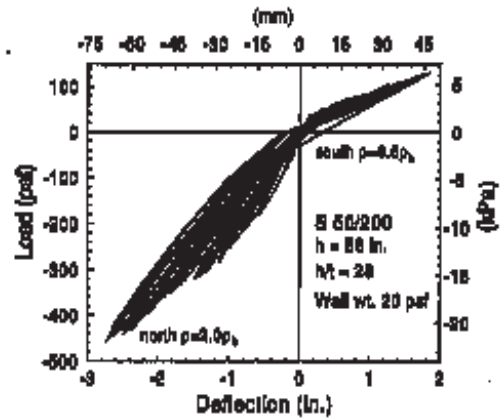
Fig. 8 Shear failure along the bottom brick course of Specimen S300/300.

Delaminated areas reached more than 75% of the area of the composite strips by the end of the test. Longitudinal strain in excess of 1.1% was measured on composite fabric on both wall faces. It is important to remark that the ratios of the applied pressure on both faces for the first major crack, first delamination, and the ultimate load were proportional to the reinforcement ratios. Figure 9 shows typical curves for all measured parameters. The general information is described in Table 3.

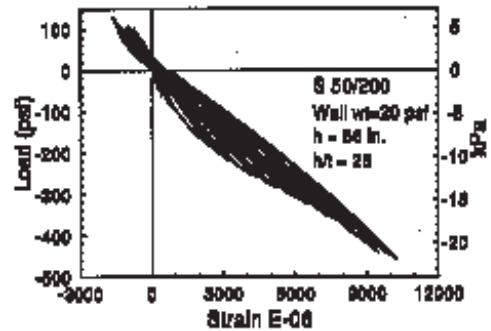
Three modes of failure were observed in this wall: tensile fracture of the composite strips on the south face, delamination on the north face, and crushing of the masonry on the south face. The tensile failure on the south face occurred on the west strip below the middle brick course. This happened although the three strips delaminated fairly symmetrically. This is attributed to the fact that the central and the east strips did not peel at midheight as the west one did. Cracks on the epoxy matrix were also observed on the central and the east strips. This indicated that a tensile failure was close to be reached.

The failure on the north face, which was reinforced with two times the balanced condition, was in combination of excessive delamination and compression of the brick. The delamination pattern at failure was nonsymmetrical. The central and the east composite strips delaminated from the top support halfway to the bottom. The west strip delaminated in opposite manner, i.e., from the bottom support halfway to the top. This delamination configuration caused a nonsymmetrical distribution of major flexural cracks. The main flexural crack was a stepped one. This was marked three bricks above the middle brick course on the east side, and stepped down to two brick courses below the middle one. In addition, another stepped crack formed above the previous one from the east side to the central composite strip. Two vertical cracks along the west and the central strips passing through the brick courses were also detected. These cracks indicate that the wall was subjected to biaxial bending; to prevent such failure, some horizontal reinforcement must be provided. It is important to note that for the first time, a clear indication of compression failure on the south face along the main stepped flexural crack was observed.

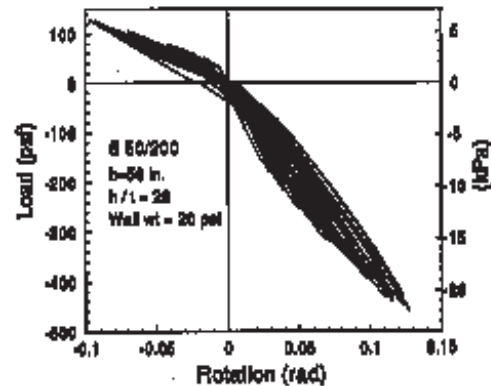
In summary, this wall was subjected to 25 and 27 cycles on the south and the north faces, respectively. The wall supported pressures equivalent to seven and 23 times its own weight for the south and the north faces. The wall was also capable to deflect on the south face as much as 18 times the maximum allowable deflection if it was unreinforced, according to the ACI/ASCE/TMS specifications. The latter is equivalent to a span drift of 3.4% ( $l/30$ ). The corresponding measured param-



(a)



(b)



(c)

Fig. 9 Typical measurements for Specimen S 50/200: (a) load versus deflection at midheight; (b) load versus the longitudinal strain in the composite strip; and (c) load versus rotation at the top support.

eters for the north face were 30 times the allowable deflection, or a span drift of 5% ( $l/20$ ). Figure 10 shows the failure of the north face and the delaminated pattern of the same face just before the failure. From the load-versus-deflection curve, it can be observed that the hysteretic loops for the north face were more enlarged. Thus, a better energy dissipating mechanism was developed on the north face.

#### Wall D100

This wall was constructed in double wythe. Because of the size of the wall and the difficulties involved in loading the wall on both faces, it was decided to retrofit the north face only. Previous tests had indicated that the reversed cyclic behavior of such walls can be fairly accurately predicted for the case of loading the wall on one side only. A reinforcement ratio equal

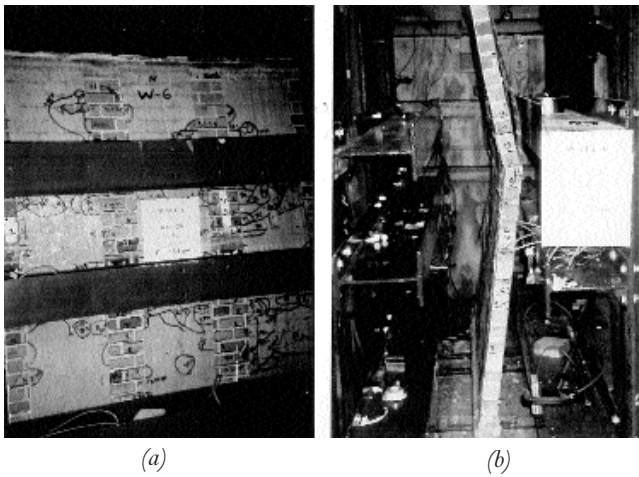


Fig. 10 Failure of the north face of Specimen S50/200: (a) delamination pattern prior to failure; (b) wall at failure.

to the balanced condition was used. A unidirectional glass fabric weighing 18 oz per  $\text{yd}^2$  was used. A header course was placed every six courses, representing approximately 16% of the wall surface. Although some mortar was placed in the vertical space separating the two wythes, due to the small size of the opening, no special attempt was made to completely fill this gap. Consequently, a full composite action could not be developed between the two wythes.

The main objective in the construction of this wall was to investigate the influence of the number of wythes in the flexural behavior of URM walls retrofitted with composites. By using a balanced reinforcement ratio, the comparison of the behavior between single and double wythe walls was also investigated between this specimen and Specimen S100/100. The wall was subjected to 24 half-cycles of loading. The salient features of the observed behavior are given as follows.

Extensive bed-joint cracking on the north face and delamination of almost 80% of the composite strips by the end of the test characterized the behavior of this wall. The maximum measured compressive strain in the bricks was 0.12%. The low compressive strain indicated that brickwork behaved elastically. Bed-joint cracks were uniformly distributed along the height of the wall. Furthermore, the gradual delamination of the composite strips prevented the development of the ultimate capacity of both materials.

The lack of full composite action between the two wythes of this wall is attributed to two factors: a) the weak interface between the wythes due to the low area represented by headers; and b) because of the partially-filled gap between the wythes. Figure 11 shows typical curves for strain and deflections. The predicted behavior by beam theory was in agreement with experimental results for deflections up to 25 mm (1.0 in.); little agreement exists for points corresponding to higher deflection levels. This deflection level is close to the first major stiffness degradation due to early delamination.

In addition to bed-joint cracks and delamination areas, two failures were detected on the wall: splitting of the wythes and sliding of the north wythe along two bed-joint cracks. These two failures were detected in the lower part of the wall. No splitting failure was detected crossing the header courses. This is due to the high interface shear capacity of headers given by the bricks. A section of the wall between the headers, however, did split. This is attributed to the low shear capacity of the poorly grouted gap. The in-plane shear capacity of the headers was calculated from the compressive strength of the brick units according to ACI/ASCE/TMS specifications to be 552 kPa (80 psi). The theoretical shear stress at the point of

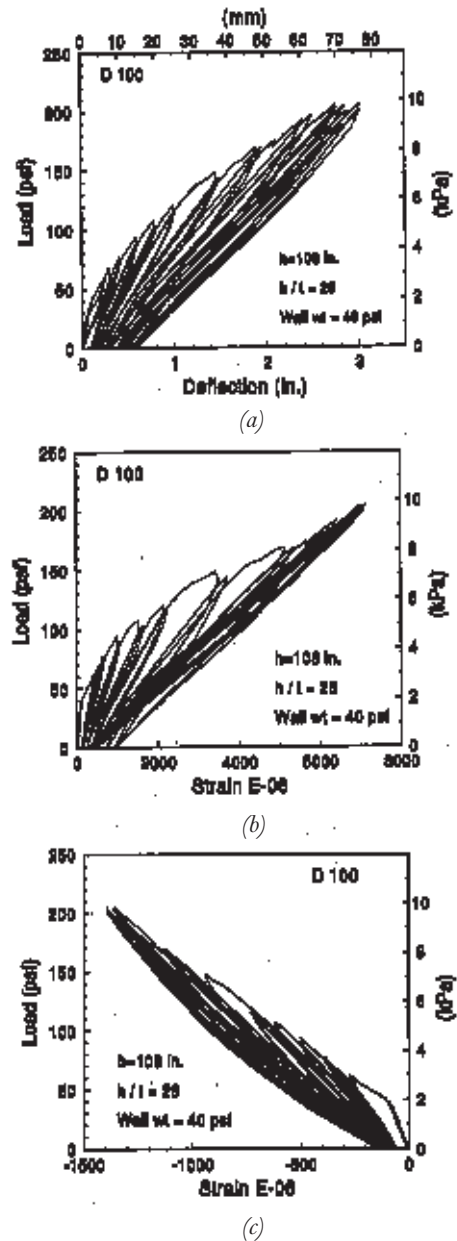


Fig. 11 Typical measurements for Specimen D100: (a) load versus deflection at mid-height; (b) load versus the longitudinal strain in the composite strip; and (c) load versus compressive strain in brick.

splitting failures calculated with elastic beam theory, assuming that the gap was fully grouted, varied from 117 to 145 kPa (17 to 21 psi); therefore, the headers did not fail in shear. These shear stresses, however, ranging from 17 to 21 psi, were beyond the shear capacity of the mortar itself. Consequently, as shown in Fig. 12, splitting cracks were observed on the east and west sides of the brick between the headers. The outward displacement of the brick, such as that shown in this figure, contributes to the delamination of the fabric. Testing of the specimen was terminated once these shear cracks were formed and the delamination reached the bottom support.

In summary, the wall behaved well although the previously mentioned failures forced a premature termination of the test. The wall was capable of deflecting a span drift of 2.77% through 24 half-cycles of loading, i.e., 17 times the allowable deflection if it was unreinforced. It also supported pressures in excess of five times its own weight. Longitudinal strains on composite strips were in agreement with those observed in

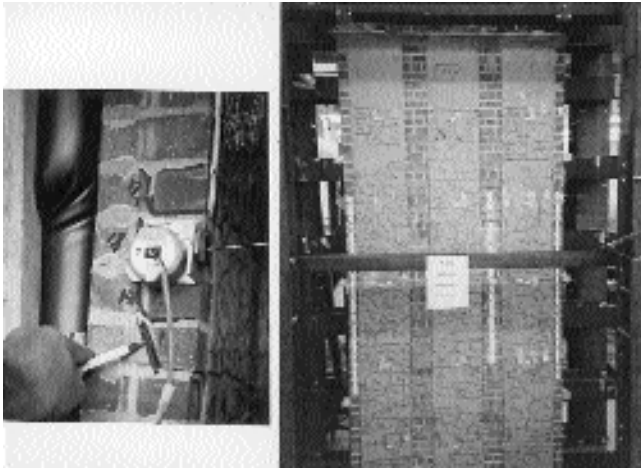


Fig. 12 Interface splitting failure and delamination pattern for Specimen D100.

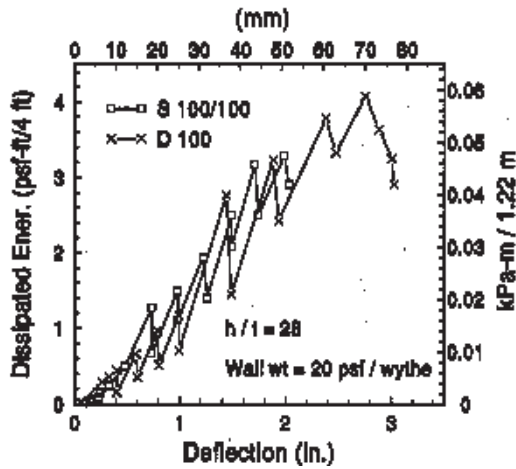


Fig. 13 Dissipated energy versus midheight deflection for Specimens S100/100 and D100.

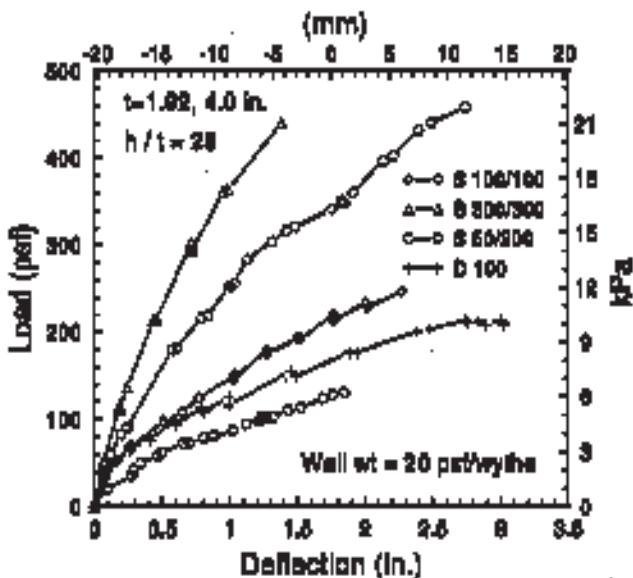


Fig. 14 Maximum load envelopes for all test specimens.

Wall S100/100. Rotations and span drifts, however, were less than 80% of the corresponding values in Specimen S100/100.

### SUMMARY OF OBSERVED BEHAVIOR

Four half-scale URM masonry walls retrofitted with vertical glass fabric composite strips were tested under cyclic out-of-plane bending. The salient parameters were the height-thickness ratio, which was held constant at 28, the number of wythes being one or two, and the reinforcement ratio that varied from 0.5 to three times that of the balanced condition. One of the tested single wythe walls was retrofitted with no primer, and the others with primer. Four types of failure were detected in walls constructed in single wythe. With the exception of Specimen S300/300 that failed due to high in-plane shear stresses along the lower brick course (i.e., more than 50 psi), the other two showed extensive delamination at failure. Tensile failure occurred for faces reinforced with half- or full-balanced condition (Table 3).

Two failure modes were detected on Wall D100. Excessive delamination took place on all composite strips, peeling off more than 80% of the areas by the end of the test. An interface shear failure, i.e., splitting of the wythes, also occurred at the lower half part along the east and the west sides. The latter was attributed to the low shear capacity of the poorly compacted mortar between the two wythes. According to the ACI/ASCE/TMS specifications and following the beam theory approach, the shear stresses caused by the applied pressure were in excess of the allowable values. No interface failure was detected along the header courses, however, since the shear capacity of the brick units was much higher than that caused by the applied pressure. The dissipated energy at different displacement levels for Walls S100/100 and D100 are compared in Fig. 13. In spite of their differences in terms of the number of wythes and the presence of a partial gap in Specimen D100, both of these specimens dissipated similar amounts of energy for displacements up to 50 mm (2.0 in.).

From Fig. 14, where the load-versus-deflection envelopes for all walls is presented, it can be observed that the maximum measured deflection did not depend too much on the amount of reinforcement. The maximum supported pressures, however, showed to be linearly dependent on the amount of reinforcement. The same trend was also observed for pressures at first visible crack, as well as for the first delaminated area. From Table 3, it can also be observed that the ultimate strain on composite strips was not dependent on the reinforcement ratio. Vertical cracks crossing the brick courses were detected on Walls S100/100 and S50/200. These failures occurred since the flexural capacity perpendicular to the bed-joint was reached. To avoid such failures in field applications, precautions must be taken by providing some reinforcement in the horizontal direction.

### CONCLUSIONS

Based on the observed failure modes, the specimens with lower reinforcement ratios exhibited a more ductile behavior. Therefore, pending further research studies, the reinforcement ratio should be limited to two times that of the balanced failure. Additional studies are also needed to examine the influence of an uneven brick surface in the development and propagation of delaminated areas. From the observed experimental behavior of the tested walls, the following conclusions can be drawn:

1. Strength and deformation capacity of the retrofitted walls were significantly enhanced; retrofitted walls resisted pressures ranging from five to 24 times the weight of the wall and deflected as much as 5% of the wall height.

2. The described retrofitting technique is very efficient since the reinforcing material (i.e., composite strips) is placed

on the surface of the wall, providing the maximum moment arm between the internal compression and tension couple.

3. The retrofitted walls failed by one of the following five modes: tension in composite fabrics, compression in brick, excessive delamination of the fabric, horizontal shear failure of the brickwork, and in the case of the double-wythe wall, interface shear failure.

4. In general, the load resisted by the specimens that caused the first major bed-joint crack, first delamination, and ultimate failure appeared to be directly proportional to the reinforcement ratio. No such correlation, however, was observed between the corresponding deflections and the reinforcement ratio.

5. In most cases, failure was controlled by peeling off of the composite strips after the specimens were subjected to a large number of loading cycles. Even in cases with high reinforcement ratios ( $\rho > \rho_b$ ), only localized signs of early compression failure were observed at the center of the wall, but no complete compression failure of the bricks occurred. Instead, failure of such specimens is often controlled by excessive delamination of the composite fabric due to the low shear transfer capacity of the brick surface; and

6. To avoid very stiff behavior and for improved hysteretic response, the reinforcement ratio should be limited to two times that of the balanced condition.

## ACKNOWLEDGEMENTS

Financial support for this study was provided under National Science Foundation (NSF) Grant No. CMS-9412950, S. C. Liu, Program Director. Velazquez-Dimas was supported through a scholarship provided by CONACYT and Universidad Autonoma de Sinaloa. These supports are gratefully acknowledged. The authors would also like to thank the contributions of undergraduate students Ryan B. Goebel, Jennifer Manning, and Gregory L. Orozco to this project. The authors would like to dedicate this paper to the memory of late Peter Boyle, Civil Engineering Shop Supervisor, for his many years of service to a number of research projects. The views expressed in this paper are those of the writers and do not necessarily represent the views of the sponsors.

## REFERENCES

ABK-TR-04, 1981, Methodology for Mitigation of Seismic Hazard in Existing Unreinforced Masonry Buildings: Wall Testing Out-of-Plane. El Segundo, Calif.

Abrams, D., and Costley, A. C., 1996, Seismic Evaluation of Unreinforced Masonry Buildings, *Paper No. 976*, Eleventh World Conference on Earthquake Engineering, Acapulco, Mexico.

Abrams, D., 1986, Lateral Resistance of a Two-Story Block Building, *Advances in Analysis of Structural Masonry*, ASCE Structures Congress, New Orleans, pp. 41-57.

Abrams, D., 1988, Dynamics and Static Testing of Reinforced Concrete Masonry Structures, *TMS Journal*, V. 17, No. 1, pp. 18-22.

Abboud, B. E.; Hamid, A. A.; and Harris, H. G., 1990, Small Scale Modeling of Concrete Block Masonry Structures, *ACI Structural Journal*, V. 87, No. 2, pp. 145-155.

Bruneau, M., 1994a, Seismic Evaluation of Unreinforced Masonry Buildings: A State-of-the-Art Report, *Canadian Journal of Civil Engineering*, V. 120, pp. 512-539.

Bruneau, M., 1994b, State-of-the-Art Report on Seismic Performance of Unreinforced Masonry Buildings, *ASCE Structural Journal*, V. 120, No. 1, pp. 230-250.

Building Code Requirements for Masonry Structures (ACI 530-95/ASCE 5-95/TMS 402-95), 1996. ACI, ASCE, and TMS, The Masonry Standards Joint Committee.

Clough, R. W.; Gulkan, P.; Manos, G. C., and Mayes, R. L., 1990, Seismic Testing of Single-Story Masonry Houses: Part I and II, *ASCE Structural Journal*, V. 116, No. 1.

Dawe, J. L., and Seah, C. K., 1998, Out-of-Plane Resistance of Concrete Masonry Infilled Panels, *Canadian Journal of Civil Engineering*, V. 16, pp. 854-864.

Dawe, J. L., and Aridru, G. G., 1993, Prestressed Concrete Masonry Walls Subjected to Uniform Out-of-Plane Loading, *Canadian Journal of Civil Engineering*, V. 20, pp. 969-979.

Drysdale, R. D.; Hamid, A. A.; and Bake, R. L., 1994, Masonry

Structures Behavior and Design, Prentice Hall.

Ehsani, M. R., and Saadatmanesh, H., 1994, Out-of-Plane Strength of Unreinforced Brickwork Retrofitted with Fiber Composites, *Proceedings, NCEER Workshop on Seismic Response of Masonry Infills*, San Francisco, Calif.

Ehsani, M. R., and Saadatmanesh, H., 1996, Seismic Retrofitting of URM Walls with Fiber Composites, *The Masonry Society Journal*, V. 14, No. 2, pp. 63-72.

Ehsani, M. R., and Saadatmanesh, H., 1997, Method of Strengthening Masonry and Concrete Walls with Composite Strap and High-Strength Random Fibers, *U.S. Patent No. 5,640,825*, United States Patents and Trademark Office, Washington, D.C.

Ehsani, M. R.; Saadatmanesh, H.; and Velazquez-Dimas, J. I., 1999, Behavior of Retrofitted URM Walls under Simulated Earthquake Loading, *ASCE Journal of Composites for Construction*, V. 3, No. 3, pp. 134-142.

Essaway, A. M., 1986, Strength of Hollow Concrete Block Masonry Walls Subjected to Lateral (Out-of-Plane) Loading, PhD thesis, McMaster University, Canada.

Hendry, A. W., 1973, The Lateral Strength of Unreinforced Brickwork, *The Structural Engineer*, V. 51, pp. 43-50.

Kehoe, B. E., 1996, Performance of Retrofitted Unreinforced Masonry Buildings, *Paper No. 1417*, Eleventh World Conference on Earthquake Engineering, Acapulco, Mexico.

Laursen, P. T.; Seible, F.; Hegemier, G. A.; and Innamorato, D., 1995, Seismic Retrofit and Repair of Masonry Walls with Carbon Overlays, *Non-Metallic (FRP) Reinforcement for Concrete Structures*, Rilem.

Lawrence, F. K., 1984, Shotcrete Strengthening of Brick Masonry Walls, *Concrete International*, V. 6, No. 7, July, pp. 34-40.

Lester, J., 1998, Staking Your Claim, *Civil Engineering*, July, pp. 65-67.

Mengy, Y., and McNiven, H., 1989, A Math Model for the In-Plane Non-Linear Earthquake Behavior of Unreinforced Masonry Walls, Part 1: Experiment and Proposed Model, *Earthquake Engineering and Structural Dynamic Journal*, V. 18, No. 5, pp. 249-261.

Prawel, S. P., and Reinhorn, A. M., 1985, Seismic Retrofit of Structural Masonry Using a Ferrocement Overlay, *Proceedings Third North American Masonry Conference*, University of Texas at Arlington, pp. 59.2-59.19.

Reinhorn, A. M.; Prawel, S. P.; and Jia, Z., 1985, Experimental Study of Ferrocement as a Seismic Retrofit Materials for Masonry Walls, *Journal of Ferrocement*, V. 15, No. 3, pp. 247-260.

Reinhorn, A. M., and Madan, A., 1995, Evaluation of TYFO-W Fiber Wrap System for Out-of-Plane Strengthening of Masonry Walls, *Report No. 95-AMR-0001*, Department of Civil Engineering, State University of New York, Buffalo, N.Y.

Saadatmanesh, H., and Ehsani, M. R., 1996, Fiber Composites in Infrastructure, *Proceedings of the First International Conference on Composites in Infrastructure (ICCI 96)*, Tucson, Ariz., 1231 pp.

Saadatmanesh, H., and Ehsani, M. R., 1998, Fiber Composites in Infrastructure, *Proceedings of the Second International Conference on Composites in Infrastructure (ICCI 98)*, Tucson, Ariz., V. I and II, 1506 pp.

Schwegerler, G., and Kelterborn, P., 1996, Earthquake Resistance of Masonry Structures Strengthened with Fiber Composites, *Paper No. 1460*, Eleventh World Conference on Earthquake Engineering, Acapulco, Mexico.

Sinha, B. P.; Maurenbrecher, A. H. P.; and Hendry, A. W., 1970, Model and Full Scale Tests on a Five-Story Cross-Wall Structure under Lateral Loading, *Proceedings, 2nd International Brick Masonry Conference, Stoke-on-Trent*, pp. 201-208.

Sucougulu, H., and McNiven, H. D., 1991, Seismic Shear Capacity of Reinforced Masonry Piers, *ASCE Structural Engineering Journal*, V. 117, No. 7, pp. 2166-2186.

Sucougulu, H., and Erberik, A., 1997, Performance Evaluation of Three-Story Unreinforced Masonry Building during the 1992 Erzincan Earthquake, *Earthquake Engineering and Structural Dynamics*, V. 26, pp. 319-339.

Sveinsson, B. I.; Blondet, M.; and Mayes, R. L., 1988, Out-of-Plane Dynamic Response of Clay Masonry Walls, *Proceedings of 57th Structural Engineers Association of California Convention*.

Velazquez-Dimas, J. I.; Ehsani, M. R.; and Saadatmanesh, H., 1998, Cyclic Behavior of Retrofitted URM Walls, *Proceedings ICII-98*, Tucson, Ariz., pp. 328-340.

Velazquez-Dimas, J. I., 1998, Out-of-Plane Cyclic Behavior of URM Walls Retrofitted with Fiber Composites, PhD dissertation, University of Arizona.

Velazquez-Dimas, J. I., and Ehsani, M. R., 2000, Modeling the Behavior of URM Walls Retrofitted with Fiber Composites, to appear in *ASCE Journal of Composites for Construction*.